Free Form Deformation with Scattered Data Interpolation Methods

Detlef Ruprecht and Heinrich Müller *

Abstract

Free form deformation has applications in computer animation, in data acquisition, and in computer aided geometric design. One approach is to deform the space in order to induce a deformation of an embedded object. A new method of this class is proposed which is based on scattered data interpolation. The usefulness of two selected classes of scattered data interpolation methods in this context is analyzed, with emphasis on the two-dimensional case. It turns out that suitable scattered data methods do exist, and that the new approach should compete well with more complex, computationally expensive physically based models.

Keywords: Geometric modelling, computer animation, deformation, scattered data interpolation.
Published in: G. Farin, H. Hagen and H. Noltemeier (eds.). *Geometric Modelling (Computing Suppl. 8)*, pages 267–281. Springer Verlag, Wien 1993.

1 Free Form Deformation

Suppose we are given an image of two-dimensional geometric objects. The task is to distort the image irregularly.

In the physical world, this goal can be reached by drawing the image on an elastic skin. The elastic skin is deformed by moving some of its points into a new position. This causes a deformation of the image too.

In a computer, the elastic skin, the image drawn on it, and the input of the points to be moved can be easily modeled by an interactive program. The user interface of such a program is shown in fig. 1. Besides some menus it consists of two neighboring rectangular regions. The left region shows the image before transformation, in the example a digitized cross section of a blossom. If a second image is known which is to be used as a target for the deformation, it can be displayed in the right region. The example in fig. 1a shows another cross section of the blossom at a later stage of evolution. By consecutively choosing a point in the left and a point in the right region, pairs of an original point and its image under the deformation to be carried out are defined. This displacement of control points is displayed by dashed lines. The calculation of the deformation is initiated

*Institut für Informatik, Universität Freiburg, Rheinstr. 10–12, W-7800 Freiburg i.Br.
E-mail: [ruprecht|mueller]@informatik.uni-freiburg.de

by selecting a corresponding menu item. The resulting deformed picture is then displayed in the right region, overlaid over the second image if one is present as shown in fig. 1b.

The images deformed in this paper consist of polygonal chains. The deformed picture is obtained by calculating the images under deformation of points on the polygonal chains and then connecting them by line segments in the same way as in the original picture. It is not too difficult to deform raster images too. A possibility is to use a look–up table with positions of pixels of the initial picture as it was done in [Wolberg, Boult, 1989].

An immediate application of image deformation is in two-dimensional computer animation. A given drawing can be animated by continuous transformation. Usually, the animation will not be designed by extrapolating an initial image, but by interpolating between two given keyframes. In applying the technique of deformation, interpolation can be performed approximately by deforming the first keyframe so that it coincides with the second as well as possible, as it was done in fig. 1. The intermediate frames required for animation may then be obtained by linear interpolation between the first keyframe and its deformation. Let $\mathbf{p}$ be a point in the first keyframe, $\mathbf{f} : \mathbb{R}^2 \rightarrow \mathbb{R}^2$ the function describing the deformation. Then the location of $\mathbf{p}$ at time t, $0 < t < 1$, is $(1 - t) \cdot \mathbf{p} + t \cdot \mathbf{f}(\mathbf{p})$.

The initial motivation for the work reported on here was a problem of geometric design. A widely used technique of solid modeling is the reconstruction of the surface of a solid from cross sections. Reconstruction from cross sections finds its application in particular in the acquisition of existing solid structures by techniques of tomography. Tomography is used in medicine, but also in microscopy or geology. One of the most powerful approaches of reconstruction is that of [Boissonnat, 1988]. This approach is based on nearest-neighbor heuristics, and is thus able to interconnect even multiple contours including branches in a usually quite likely way. However, troubles arise if the cross sections are highly dissimilar. The blossoms of fig. 1 are an example if the time axis is taken as the third spatial axis. Free form deformation allows a distortion of the cross sections with only a few assignments so that Boissonnat's algorithm may find a reconstruction between the deformed cross sections. The actual reconstruction is obtained by back-transformation which can simply be achieved by replacing the deformed coordinates by the original ones. In this manner, a good reconstruction from the original cross sections can often be achieved.

Another problem with techniques of tomography is that their physical properties often cause distortions of the cross sections during catching [Buche, Camillerapp, 1991]. For their correction, free form deformation can be used as well. A last example of an application is the design of free form solids in computer aided geometric design by deforming initially simple solids into complex shapes [Sederberg, Parry, 1986].

The crucial question not addressed yet is the calculation of the deformation. One possibility is the correct simulation of a physical model, for example an elastic skin of rubber. Such models have found application in e.g. face modeling [Guenther, 1989]. These approaches seem to be expensive. In the following a more simple method is proposed. The problem of deformation is interpreted as a problem of interpolation. It turns out that deformation is closely related to the problem of scattered data interpolation. This opens the possibility to refer to well-known techniques in this area [Franke, 1982, Alfeld, 1989]. From the high number of scattered data methods, we have chosen two types for our investigations, the classic Shepard approach with some modifications and interpolation with radial basis functions, in particular Hardy's multiquadrics. The experimental investigations show that with this approach good results can be achieved as long as the

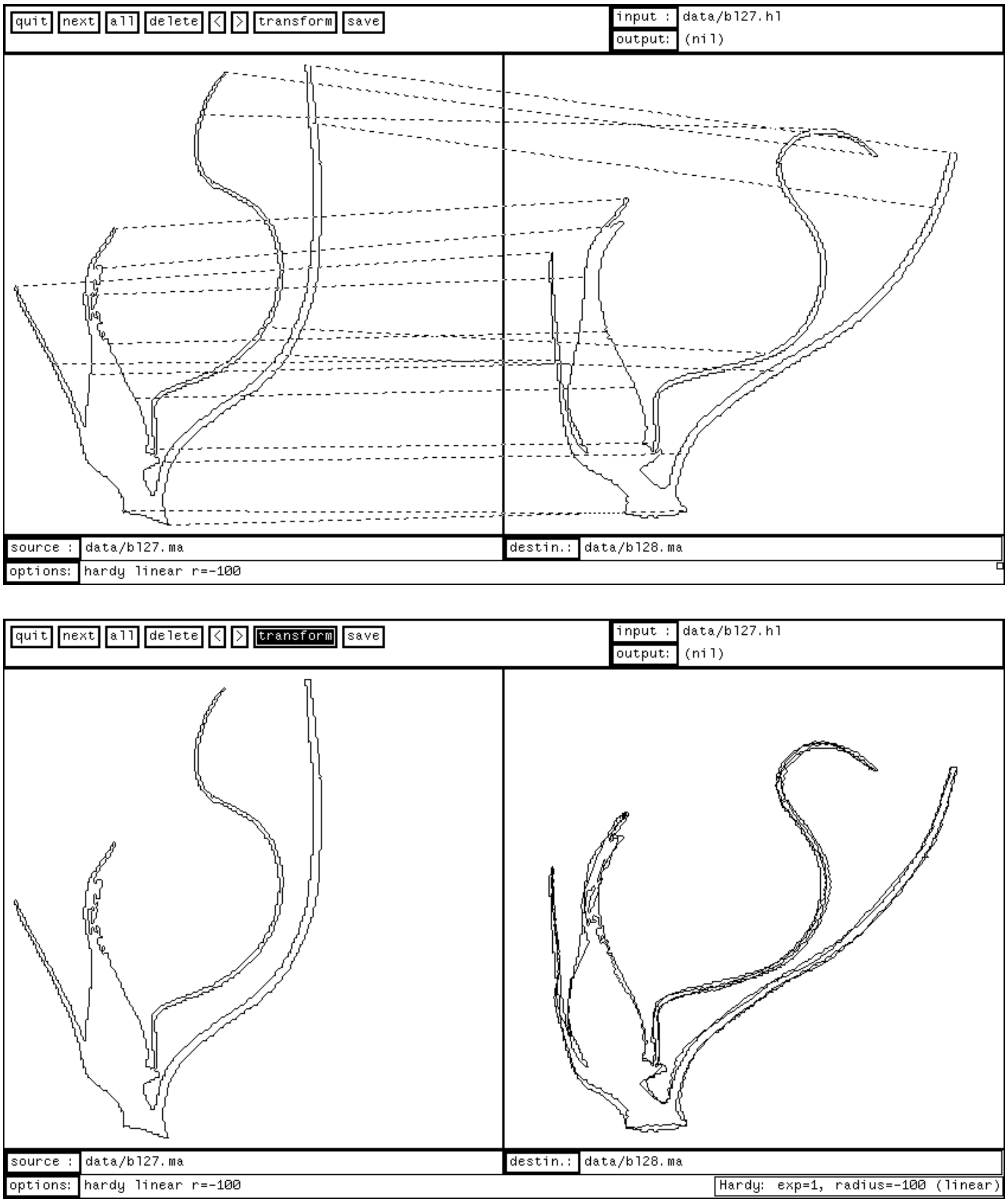

Figure 1: Deformation of a cross section of a blossom. The upper picture shows two given states of evolution of the blossom and an assignment for deformation. In the right region of the picture below the original second state and the deformation of the first state calculated from the assignment are displayed simultaneously.

dissimilarity between the original image and that endeavored by deformation is not too high. A first impression can be got from Fig. 1, in which interpolation with multiquadrics is used. Despite the low number of assignments, the similarity of both pictures is convincing. Bigger deformations can be performed by decomposition into a sequence of smaller deformations.

The remainder of this contribution is organized as follows. In sect. 2 the relation between the problem of deformation and the problem of scattered data interpolation is established. The scattered data methods and their behavior for the problem of deformation are the subject of sect. 3 and 4. Piecewise deformation is discussed in sect. 5. A comparison between the two approaches of scattered data interpolation, as well as with other methods of deformation known in literature is performed in sect. 6.

2 Deformation and Scattered Data Interpolation

The problem of deformation can be formulated as follows.

Deformation Problem.
Input: n pairs $(\mathbf{p}_i, \mathbf{q}_i)$ of control points, $\mathbf{p}_i, \mathbf{q}_i \in \mathbb{R}^d$, $i = 1, \ldots, n$.
Output: An at least continuous function $\mathbf{f} : \mathbb{R}^d \to \mathbb{R}^d$ with $\mathbf{f}(\mathbf{p}_i) = \mathbf{q}_i$.

For the image deformation problem we have $d = 2$. Besides continuity, other properties of the function $\mathbf{f}$ are desirable which concern the visual pleasantness and which are hard to describe in an exact manner. These properties will become recognizable in the following discussion of concrete propositions.

The problem of scattered data interpolation is to find a real valued multivariate function interpolating a finite set of irregularly located data points.

Scattered Data Interpolation Problem.
Input: n data points $(\mathbf{x}_i, y_i)$, $\mathbf{x}_i \in \mathbb{R}^d$, $y_i \in \mathbb{R}$, $i = 1, \ldots, n$.
Output: An at least continuous function $f : \mathbb{R}^d \to \mathbb{R}$ interpolating the given data points, i.e. $f(\mathbf{x}_i) = y_i$, $i = 1, \ldots, n$.

Scattered data methods can now be simply used by interpolating each component $f_j : \mathbb{R}^d \to \mathbb{R}$, $j = 1, \ldots, d$, of $\mathbf{f}$ separately. The data points to be used are $(\mathbf{p}_i, q_{i,j})$, $q_{i,j}$ the j-th component of $\mathbf{q}_i$.

3 Shepard Interpolation

The Shepard approach of scattered data interpolation [Shepard, 1968] uses a weighted average of the data values at the data points, with weights dependent on the distance of the observed point from the given data points,

$$f(\mathbf{x}) \quad = \quad \sum_{i=1}^{n} w_i(\mathbf{x}) y_i. \tag{1}$$

$w_i : \mathbb{R}^n \to \mathbb{R}$ is the weight function and $y_i \in \mathbb{R}$ the data value at the data point $\mathbf{x}_i \in \mathbb{R}^d$. The weight functions satisfy the conditions

$$w_i(\mathbf{x}) \;\; \geq \;\; 0, \quad i = 1, \ldots, n, \quad \sum_{i=1}^{n} w_i(\mathbf{x}) = 1, \quad \text{and} \tag{2}$$

$$w_i(\mathbf{x}_j) \;\; = \;\; \delta_{ij}, \quad \text{i.e.} \quad w_i(\mathbf{x}_i) = 1 \quad \text{and} \quad w_i(\mathbf{x}_j) = 0, \quad j \neq i, \; i, j = 1, \ldots, n. \tag{3}$$

These conditions guarantee the property of interpolation.

In [Shepard, 1968] the following weight function was proposed,

$$w_i(\mathbf{x}) = \frac{\sigma_i(\mathbf{x})}{\sum_{j=1}^{n} \sigma_j(\mathbf{x})}\text{, with} \tag{4}$$

$$\sigma_i(\mathbf{x}) = \frac{1}{(d_i(\mathbf{x}))^{\mu}}, \quad d_i(\mathbf{x}) \text{ the distance between } \mathbf{x} \text{ and } \mathbf{x}_i. \tag{5}$$

The smoothness is determined by the exponent μ. $\mu > 1$ assures the continuity of the first derivative, its value disappears at the data points.

The Shepard interpolation in this form shows an unfavorable behavior when applied to the problem of deformation. Using the weighted average of the given control points causes all other points to be shifted towards the geometric center of the displaced control points. Fig. 2a shows the example of a square grid whose four corners are fixed. No further assignments were given apart from these four pairs of identical points. The original grid is shown with dashed lines, the deformation with solid lines. The created image is considerably distorted, which means that a simple Shepard approach will usually not be well suited for the application to deformation.

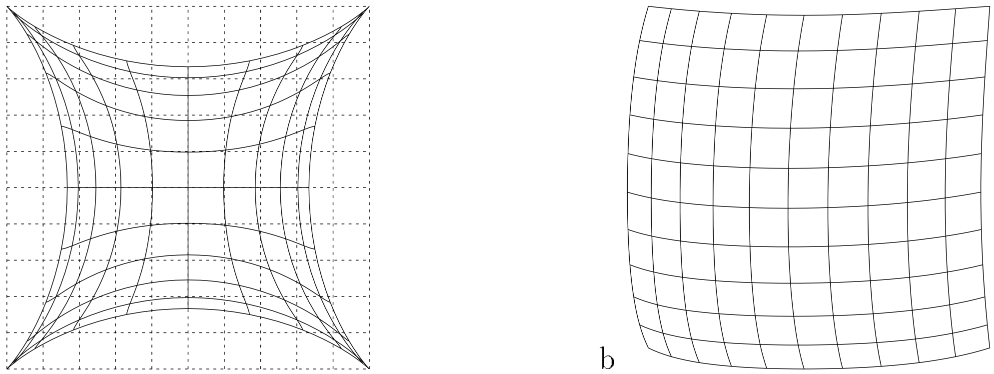

Figure 2: Deformation of a square grid with fixed corners: (a) simple Shepard approach; (b) radial basis functions with Hardy's multiquadrics without polynomial.

3.1 Local interpolants

Several authors, among them [Gordon, Wixom, 1978, Franke, 1980, Lancaster, Salkauskas 1981, Farwig, 1986], have proposed modified approaches which replace the value y_i in Shepard's formula by a local interpolant $f_i(\mathbf{x}) : \mathbb{R}^n \rightarrow \mathbb{R}$,

$$f(\mathbf{x}) = \sum_{i=1}^{n} w_i(\mathbf{x}) f_i(\mathbf{x}), \quad f_i(\mathbf{x}_i) = y_i, \ i = 1, \ldots, n. \tag{6}$$

[Franke,1980] proposed to compute the local interpolant $f_i(\mathbf{x})$ by minimizing the squared error of the mapping of all other control points $\mathbf{x}_j$ with f_i, weighted with a coefficient w_{ij} to attenuate the influence of distant points. The corresponding error function $E_i(f)$ is

$$E_i(f) = \sum_{j=1, j\neq i}^{n} w_{ij} \cdot \|f(\mathbf{x}_j) - y_j\|^2. \tag{7}$$

The optimum local interpolant is obtained by minimizing $E_i(f)$. The coefficients w_{ij} should depend on the distance between $\mathbf{x}_i$ and $\mathbf{x}_j$ in a manner similar to $w_i(\mathbf{x})$, but it is not possible to use w_i because of (3). A simple possibility is to use $w_{ij} = \sigma_i(\mathbf{x}_j)$. This approach has been used in our examples on local interpolants.

The application of (6) to the problem of deformation leads to

$$\mathbf{f}(\mathbf{p}) = \sum_{i=1}^{n} w_i(\mathbf{p})\mathbf{f}_i(\mathbf{p}), \quad \mathbf{f}_i(\mathbf{p}_i) = \mathbf{q}_i, \; i = 1, \ldots, n. \tag{8}$$

$\mathbf{f}_i : \mathbb{R}^d \to \mathbb{R}^d$ are the local interpolants. They can be rewritten as

$$\mathbf{f}_i(\mathbf{p}) = \mathbf{q}_i + \mathbf{D}_i(\mathbf{p} - \mathbf{p}_i), \text{ with } \mathbf{D}_i : \mathbb{R}^d \to \mathbb{R}^d, \ \mathbf{D}_i(0) = 0. \tag{9}$$

A simple possibility is to choose the $\mathbf{D}_i$ as linear transformations. Then $\mathbf{D}_i$ can be represented by a $d \times d$–matrix $(d_{i,kl})$, $k, l = 1, \ldots, d$. In the two-dimensional case the error function corresponding to a linear transformation $\mathbf{D}$ is

$$\begin{aligned} E_i(\mathbf{D}) &= \sum_{j=1, j\neq i}^{n} w_{ij} \cdot \|\mathbf{q}_i + \begin{pmatrix} d_{11} & d_{12} \\ d_{21} & d_{22} \end{pmatrix} (\mathbf{p}_j - \mathbf{p}_i) - \mathbf{q}_j\|^2 & (10) \\ &= \sum_{j=1, j\neq i}^{N} w_{ij}[(d_{11}(p_{j,1} - p_{i,1}) + d_{12}(p_{j,2} - p_{i,2}) + q_{i,1} - q_{j,1})^2 + \\ &\quad +(d_{21}(p_{j,1} - p_{i,1}) + d_{22}(p_{j,1} - p_{i,1}) + q_{i,2} - q_{j,2})^2]. & (11) \end{aligned}$$

The minimum of the error function is obtained with the partial derivatives with respect to the d_{kl}, $k, l = 1, 2$. For $\partial E_i(\mathbf{D})/\partial d_{11}$, for example, we have

$$\begin{aligned} \frac{\partial E_i(\mathbf{D})}{\partial d_{11}} &= \sum_{j=1, j\neq i}^{n} w_{ij}[2d_{11}(p_{j,1} - p_{i,1})^2 + 2d_{12}(p_{j,1} - p_{i,1})(p_{j,2} - p_{i,2}) + \\ &\quad +2(q_{i,1} - q_{j,1})(p_{j,1} - p_{i,1})]. \end{aligned} \tag{12}$$

Hence the derivatives are linear functions of the $d_{i,kl}$. Their second derivatives show that the zeros of the first derivative are indeed a minimum. Thus a linear system of four equations with four unknowns is obtained. The system has a unique solution if its determinant is not equal to zero. The solutions are

$$\begin{aligned} det_i &= (\sum_{j=1, j\neq i}^{n} w_{ij}(p_{j,1} - p_{i,1})^2)(\sum_{j=1, j\neq i}^{n} w_{ij}(p_{j,2} - p_{i,2})^2) - \\ &\quad -\Big[\sum_{j=1, j\neq i}^{n} w_{ij}(p_{j,1} - p_{i,1})(p_{j,2} - p_{i,2})\Big]^2 & (13) \\ d_{i,11} &= \frac{1}{det_i}\Big[(\sum w_{ij}(q_{j,1} - q_{i,1})(p_{j,1} - p_{i,1}))(\sum w_{ij}(p_{j,2} - p_{i,2})^2) - \\ &\quad -(\sum w_{ij}(q_{j,1} - q_{i,1})(p_{j,2} - p_{i,2}))(\sum w_{ij}(p_{j,1} - p_{i,1})(p_{j,2} - p_{i,2}))\Big] & (14) \\ d_{i,12} &= \frac{1}{det_i}\Big[(\sum w_{ij}(q_{j,1} - q_{i,1})(p_{j,2} - p_{i,2}))(\sum w_{ij}(p_{j,1} - p_{i,1})^2) - \\ &\quad -(\sum w_{ij}(q_{j,1} - q_{i,1})(p_{j,1} - p_{i,1}))(\sum w_{ij}(p_{j,1} - p_{i,1})(p_{j,2} - p_{i,2}))\Big] & (15) \end{aligned}$$

$$
\begin{aligned}
d_{i,21} &= \frac{1}{det_i}\Big[(\sum w_i(\mathbf{p}_j)(q_{j,2}-q_{i,2})(p_{j,1}-p_{i,1}))(\sum w_{ij}(p_{j,2}-p_{i,2})^2) - \\
&\quad -(\sum w_{ij}(q_{j,2}-q_{i,2})(p_{j,2}-p_{i,2}))(\sum w_{ij}(p_{j,1}-p_{i,1})(p_{j,2}-p_{i,2}))\Big] \qquad (16) \\
d_{i,22} &= \frac{1}{det_i}\Big[(\sum w_{ij}(q_{j,2}-q_{i,2})(p_{j,2}-p_{i,2}))(\sum w_{ij}(p_{j,1}-p_{i,1})^2) - \\
&\quad -(\sum w_{ij}(q_{j,2}-q_{i,2})(p_{j,1}-p_{i,1}))(\sum w_{ij}(p_{j,1}-p_{i,1})(p_{j,2}-p_{i,2}))\Big]. \qquad (17)
\end{aligned}
$$

If $det_i = 0$, a simpler local interpolant with $d_{i,11} = d_{i,22}$ and $d_{i,12} = -d_{i,21}$ is used which allows uniform scaling and rotation, but no shearing. The $d_{i,kl}$ are again calculated by minimizing $E_i(\mathbf{D})$ with the result

$$
\begin{aligned}
d_i &= \sum w_{ij}((p_{j,1}-p_{i,1})^2 + (p_{j,2}-p_{i,2})^2) \qquad (18) \\
d_{i,11} &= d_{i,22} = \frac{1}{d_i}\sum w_{ij}((p_{j,1}-p_{i,1})(q_{j,1}-q_{i,1}) + (p_{j,2}-p_{i,2})(q_{j,2}-q_{i,2})) \qquad (19) \\
d_{i,12} &= -d_{i,21} = \frac{1}{d_i}\sum w_{ij}((p_{j,2}-p_{i,2})(q_{j,1}-q_{i,1}) - (p_{j,1}-p_{i,1})(q_{j,2}-q_{i,2})) \qquad (20)
\end{aligned}
$$

If even this cannot be computed, $\mathbf{D}_i$ is set to an identical transformation.

With a linear local interpolant, the interpolation has linear precision, i.e. if the requested displacements can be satisfied by a linear transformation, this is what will be obtained. For example, a deformation as in fig. 2, where all control points retain their initial position, will exactly reproduce the initial image.

The examples in figs. 3–5 demonstrate the effect of the deformation. To make comparison easier, various examples of the deformation of a 10×10 square grid are shown. Examples of modeling applications are also given. The same set of displacement assignments for the control points is used throughout each figure. For clarity, the original image and the displacements are only shown in the first example in each figure.

Fig. 3a shows a square grid with fixed corners within which a 2×2 square has been turned clockwise by 45°. The original grid is displayed with dashed lines and the displacement assignments with solid lines. Fig. 3b shows the result of Shepard deformation with $\mu = 2$. The waviness of the edges of the inner square comes from the influence of the fixed corner points of the grid. Increasing μ reduces this waviness, as the influence of the corner points is reduced. Similarly, the grid edges are pulled along by the rotation of the inner square. As some points along the grid edges are actually closer to the inner square than to the corner points, increasing μ does not help here. Fig. 3c shows the deformation with $\mu = 3$.

Fig. 4a and 4b show the same square grid deformed into a side-view of a head. Fig. 4a uses $\mu = 2$, fig. 4b uses $\mu = 3$. The method reacts to the input of displacements in an intuitive and straightforward manner. Note the differences caused by the different range of influence of the control points.

Fig. 5a shows a straight bar which is deformed into a telephone handset with $\mu = 2$. The produced image is not very satisfying. The observed unevenness near the data points is typical for the Shepard approach. Therefore it is better suited for applications where some jaggedness is desirable – as in the head shown in fig. 4 – than for applications needing smooth deformations as is common in Computer Aided Geometric Design.

Higher order polynomials can be used as well. [Franke, Nielson, 1980] recommend the use of second order polynomials. This does not appear to be necessary in the case of deformation. Also, higher order polynomials tend to introduce oscillations which may be acceptable in data interpolation, but undesirable for deformation.

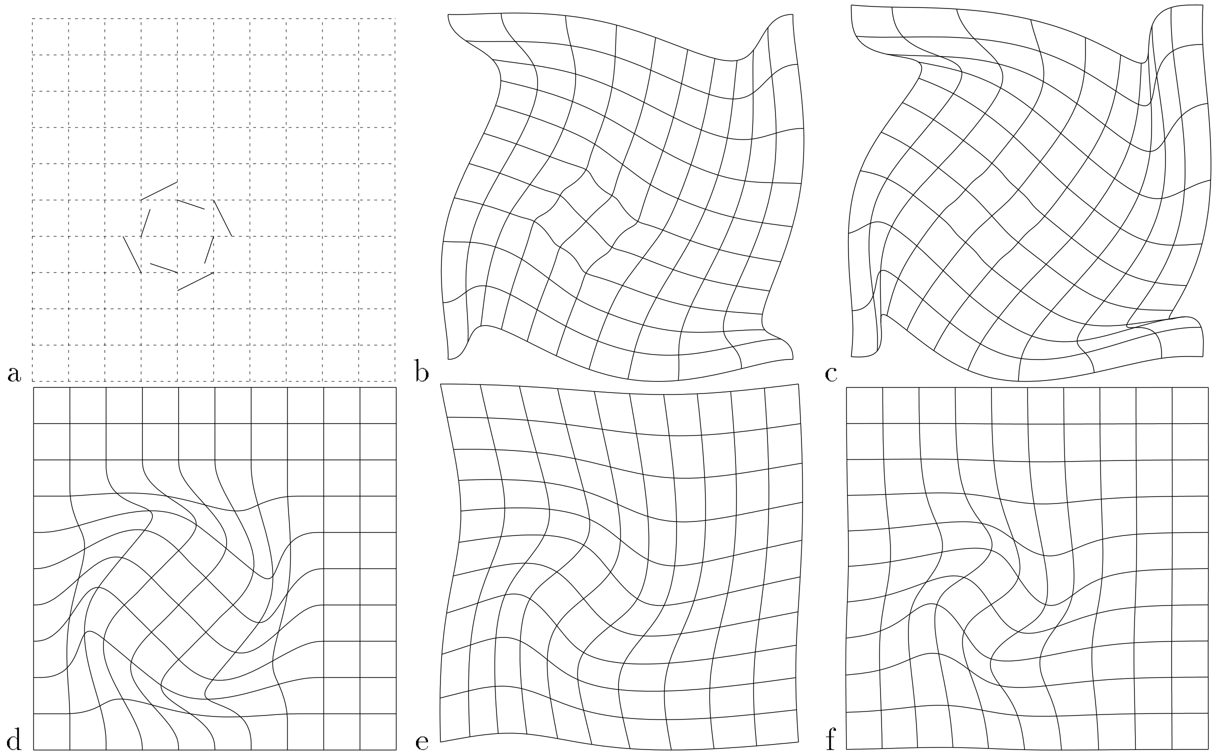

Figure 3: Rotating an embedded 2×2–square by 45° within a square grid with fixed corners: (a) Original grid with displacements; (b) Shepard with local interpolation ($\mu = 2$); (c) Shepard with local interpolation ($\mu = 3$); (d) Shepard with weight functions with limited influence ($r = 3$, $\sigma_0 = 1$); (e) Hardy's multiquadrics ($\mu = 1$); (f) Hardy's multiquadrics with limited influence ($r = 3$, $\mu = -8$).

3.2 Relaxing the Interpolation Condition

The smoothness of the deformation can be improved by adding a damping term $c > 0$ to the weight function (5), i.e.

$$\sigma_i(\mathbf{x}) \quad = \quad \frac{1}{(d_i(\mathbf{x}) + c)^\mu}. \tag{21}$$

With this weight function, exact interpolation is not provided, but with c sufficiently small the approximation follows the intention specified in the control point displacements quite well. Fig. 4c demonstrates this for a value of $c = 0.1$. This image is noticeable smoother than the images in fig. 4a and b.

An individual c_i could be specified for each data point, so that the user can specify the desired precision for each control point. This, however, would make the input of displacements more cumbersome.

With $c < 0$, strict adherence to the local interpolant can be enforced for $d_i(\mathbf{x}) \leq c$. This might be useful if special conditions, e.g. conservation of area or angles, have to be met in the vicinity of the control points.

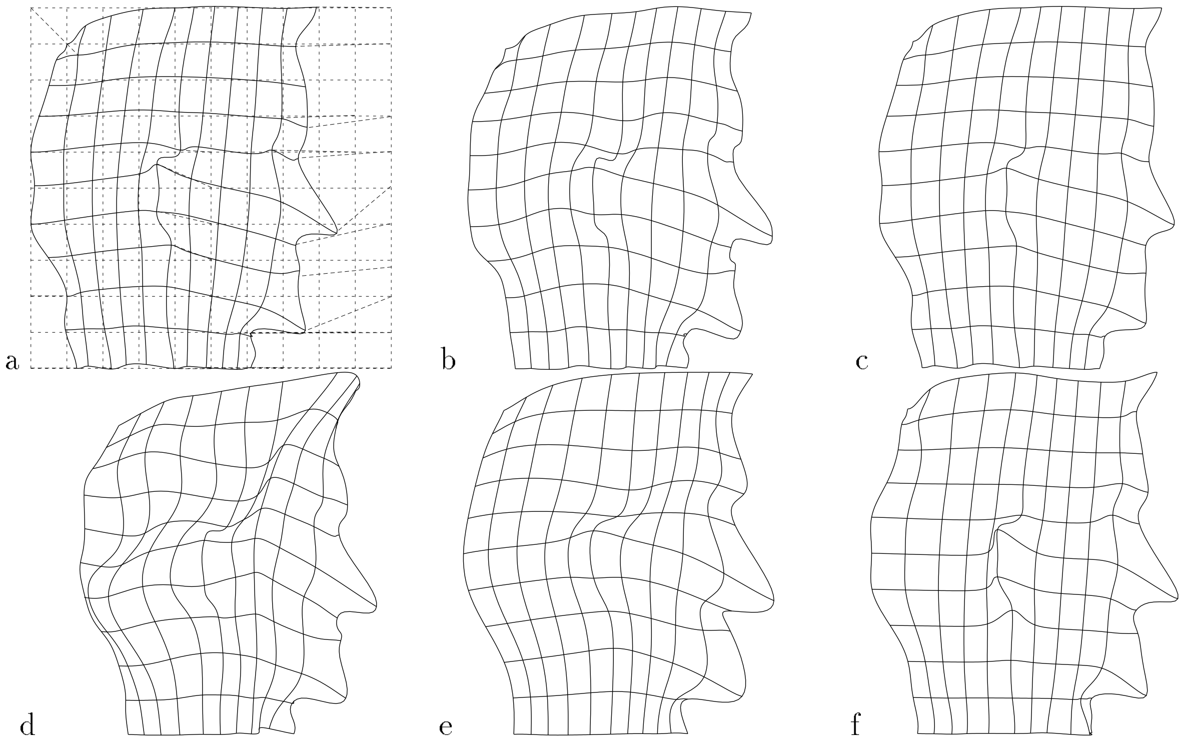

Figure 4: Deformation of a square grid into a head: (a) Shepard with local interpolation ($\mu = 2$); (b) Shepard with local interpolation ($\mu = 3$); (c) Shepard with damping ($\mu = 2$, $c = 0.1$); (d) Shepard with limited influence ($r = 5$, $\sigma_0 = 0.1$); (e) Hardy's Multiquadrics ($\mu = 1$); (f) Hardy's Multiquadrics with limited influence ($\mu = -5$).

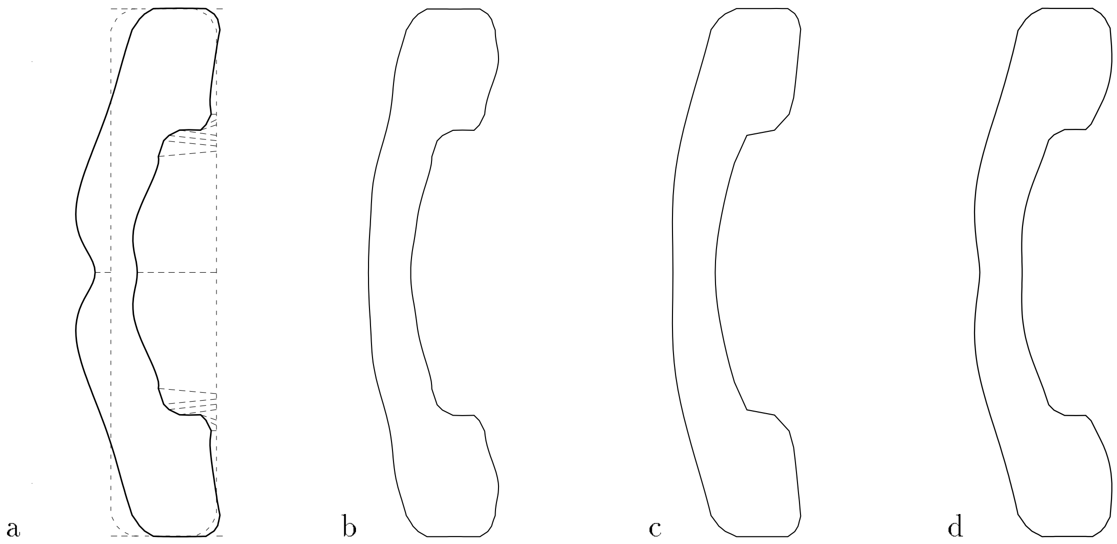

Figure 5: Deformation of a straight bar to a telephone handset: (a) Shepard with local interpolation; (b) Shepard with limited influence ($r = 3$, $\sigma_0 = 1$); (c) Hardy's Multiquadrics; (d) Radial basis function $d(\mathbf{x})^2 \log d(\mathbf{x})$.

3.3 Locally Bounded Weight Functions

If only part of an image is to be deformed, it is desirable to limit the sphere of influence of the control points, so that the deformation of a point is only influenced by control points at a distance $d_i(x) < r_i$. [Franke, Nielson, 1980] proposed the following weight function:

$$\sigma_i(\mathbf{x}) \;=\; \begin{cases} \left(\dfrac{r_i - d_i(\mathbf{x})}{r_i d_i(\mathbf{x})}\right)^{\mu} & \text{for} \quad d_i(\mathbf{x}) < r_i, \\ 0 & \phantom{\text{for}} \quad d_i(\mathbf{x}) \geq r_i. \end{cases} \tag{22}$$

In order to ensure that there is at least one non-zero weight for all points in the source image, a global function $\mathbf{f}_0(\mathbf{x})$ and a corresponding weight $\sigma_0(\mathbf{x})$ should be added to (4) and (8) so that

$$\mathbf{f}(\mathbf{p}) \;=\; \sum_{i=0}^{n} w_i(\mathbf{p})\mathbf{f}_i(\mathbf{p}), \quad \text{with } \mathbf{f}_i(\mathbf{p}_i) = \mathbf{q}_i,\ i = 1, \ldots, n \quad \text{and} \tag{23}$$

$$w_i(\mathbf{x}) \;=\; \frac{\sigma_i(\mathbf{x})}{\sum_{j=0}^{n} \sigma_j(\mathbf{x})}. \tag{24}$$

In the case of localized deformations, identical transformations $\mathbf{f}_0(\mathbf{x}) = \mathbf{x}$ with a constant user–selectable σ_0 perform quite well.

Fig. 3d shows the result for the rotated $2{\times}2$ square with $r = 3$ and $\sigma_0 = 1$. Areas further than 3 grid units away from the rotated square are completely unaffected by the deformation.

Fig. 4d shows the grid deformed into a head with $r = 5$ and $\sigma_0 = 0.1$. The results obtained here are unsatisfying, which is probably due to the sometimes sudden change of spheres of influence from one control point to another.

Fig. 5b shows the telephone handset produced from a straight bar with $r = 3$ and $\sigma_0 = 1$. Here the limitation of the influence of the control point has quite a positive effect on the deformation, although the result is still not perfect.

[Franke, Nielson, 1980] alternatively also propose weight functions bounded by a triangulation of the control points. This shows that there is an almost unlimited number of variations on weight functions to suit special purposes.

4 Radial Basis Functions

A further approach to scattered data interpolation is to construct the interpolant as a linear combination of basis functions and then to determine the coefficients of the basis functions,

$$f(\mathbf{x}) = \sum_{i=1}^{n} \alpha_i \; R(d_i(\mathbf{x})) + p_m(\mathbf{x}). \tag{25}$$

The values of the basis function R usually depend only on the distance from the data point, and are thus called radial. $p_m(\mathbf{x})$ is a polynomial of degree m. It assures a certain degree m of polynomial precision. The coefficients α_i are calculated by putting the data points into (25) and solving the resulting linear system of equations.

Well-known radial basis functions are *Hardy's multiquadrics* [Hardy, 1971],

$$R(d) = (d^2 + r^2)^{\mu/2} \quad \text{with} \quad r > 0 \text{ and } \mu \neq 0. \tag{26}$$

Hardy suggests to set p_m identical to 0. This implies a polynomial precision of 0. For the exponent μ, Hardy proposes $\mu = 1$. $\mu = -1$ has also been used, but is generally less stable.

$r > 0$ can be chosen arbitrarily. It determines the smoothness of interpolation at the given data points. [Eck, 1991] proposes to use individual values r_i for each data point $\mathbf{p}_i$, computed from the distance to the nearest neighbor, i.e.

$$r_i = \min_{i \neq j} d_i(\mathbf{x}_j). \tag{27}$$

This causes the deformation to be softer when data points are widely spaced and stronger when they are closer together. This approach has been used in our examples unless otherwise noted.

The application of radial basis functions to the problem of deformation gives

$$\mathbf{f}(\mathbf{p}) = \sum_{i=1}^{n} \alpha_i \ \mathbf{R}(d_i(\mathbf{p})) + \mathbf{p}_m(\mathbf{p}). \tag{28}$$

Now $\mathbf{R} : \mathbb{R} \to \mathbb{R}^d$ is a vector valued function of the distance and $\mathbf{p}_m : \mathbb{R}^d \to \mathbb{R}^d$ is a function with polynomial components of degree m.

It turns out that Hardy's multiquadrics approach without a polynomial term $\mathbf{p}_m$ does not yield satisfactory results as it produces distortions even with the simple transformation of a square grid with fixed corners, as shown in fig. 2b. This behavior is caused by the non-linearity of the basis functions. Introducing a linear $\mathbf{p}_m$, i.e. $m = 1$, as a global approximation with coefficients computed by the least squares method overcomes the problem. With this, the example yields an identical transformation as desired.

Fig. 3e shows a rotated square inside a grid with $\mu = 1$. The deformation is much smoother than that achieved with Shepard methods. Fig. 4e shows a head created from a square grid with multiquadrics. The smoothness of the results obtained by this method is obviously not very well suited for this sort of application. Fig. 5c, however, shows that the telephone handset created from a straight bar looks very good with multiquadrics.

With a $\mathbf{p}_m$ as introduced above, it is possible to use locally bounded basis functions which disappear for $d_i(\mathbf{x}) > r_i$. This way, radial basis functions can be used for local deformations. For these applications, the identical transformation $\mathbf{p}_m(\mathbf{p}) := \mathbf{p}$ is an adequate polynomial approximation. The effect of multiquadrics with a negative exponent $\mu < -2$ is quite localized even though they are not strictly bounded basis functions. Fig. 3f shows the rotated square for $r = 3$ and $\mu = -8$. The locality of the deformation is well demonstrated. Fig. 4f shows multiquadrics with $\mu = -5$ applied to the deformation of a grid into a head. The result is better than with $\mu = 1$, although for this type of "artistic" modeling, the results of Shepard's methods are still superior.

Other radial basis functions have been proposed [Duchon, 1977] which allow a physical interpretation as a minimal thin plate functional:

$$R(d) = d^3, \quad \text{and} \tag{29}$$
$$R(d) = d^2 \cdot \log d. \tag{30}$$

In our experiments, deformations obtained from these basis functions were consistently less satisfactory than those from multiquadrics. Fig. 5d shows an example with the telephone handset for the radial basis function (30).

5 Iterated Deformation

The experiments show that in the case of small deformations good results can be achieved with many approaches. For bigger deformations, however, undesired foldover can occur in the deformed picture (fig. 6). These are caused by the fact that, contrary to the scattered data problem, the image space is mapped onto itself. The influence of the control points on a transformed point should therefore be dependent not only on the initial relative position but also on the trajectory along which a control point is moved to its new location.

Moving the control points can be simulated by decomposing the deformation into several smaller deformations which are executed sequentially. When choosing a linear trajectory, the deformation with pairs of control points $(\mathbf{p}_i, \mathbf{q}_i)$ is linearly subdivided into m deformations $(\mathbf{p}_{i,k}, \mathbf{q}_{i,k})$, $\mathbf{q}_{i,k} = \mathbf{p}_{i,k+1}$, $k = 0, \ldots, m-1$, with

$$\mathbf{p}_{i,k} = \mathbf{x}_i + \frac{k}{m} \cdot (\mathbf{q}_i - \mathbf{p}_i), \quad k = 0, ..., m. \tag{31}$$

Fig. 6a and b show a square grid with an embedded 4×4 square rotated by 90° with a non-iterated transformation and with four iterations, respectively. For the transformations, multiquadrics are used. The foldover in the non-iterated transformation is clearly visible. Note that iteration is not used in any of the other examples. The deformation in these examples is not strong enough to make this necessary.

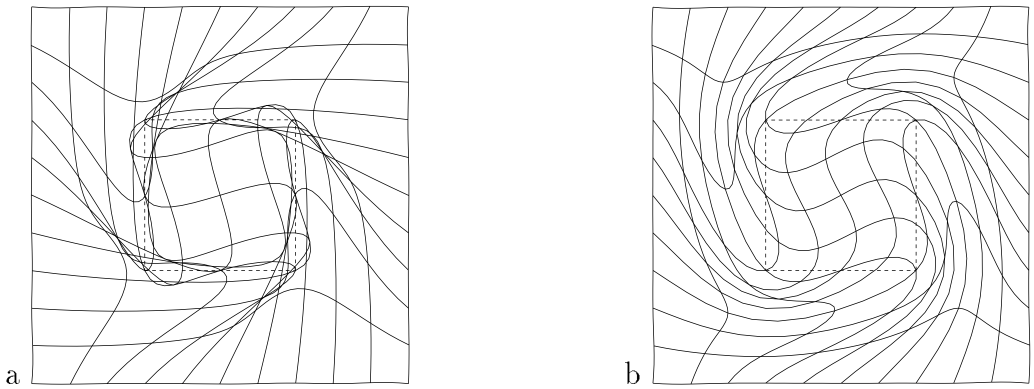

Figure 6: rotation of a 4×4 square embedded in a square grid by 90° (a) without iteration, (b) with four steps of iteration.

Splitting a deformation into a series of iterated transformations is also helpful when it is necessary to reverse the deformation. This can be done by deforming the result with the reversed control points $(\mathbf{q}_i, \mathbf{p}_i)$. To reproduce the original image well, the weights w_i, or the α_i for radial basis functions, should not change much between successive iteration steps, i.e. $w_{i,k}(\mathbf{p}_{j,k}) \approx w_{i,k+1}(\mathbf{p}_{j,k+1})$. This can always be enforced by using a sufficiently large m.

For keyframe animation, it appears to be useful to use a non-linear division of the deformation to avoid discontinuities of the movement at the keyframes.

6 Discussion

An approach for the deformation of geometric objects has been presented. The deformation is controlled by pairs of points which can be chosen arbitrarily. From these points, a function of deformation is calculated by methods derived from scattered data interpolation. The function is defined on the whole surrounding space and thus is in particular applied to any objects embedded in this space. The given points are mapped exactly while the other points follow in a natural manner dependent on the method applied.

Two classes of approaches for scattered data interpolation were investigated, the Shepard methods and the method of radial basis functions. Shepard methods have the advantage of more intuitive parameters, with the consequence that the behavior of the deformation can be easily tailored to meet specific needs. They tend to produce a somewhat jagged deformation which is often useful in artistic applications but is undesirable if smooth deformation is sought. Radial basis function methods on the other hand give very smooth and visually pleasant results as usually desired in CAGD applications and are more robust with respect to parameters. Modifying them to suit special purposes is somewhat less intuitive, however. Both approaches are easily modified to give local deformations. Both behave gracefully outside the convex hull of the control points.

In [Sederberg, Parry, 1986] an approach was described which also calculates deformations controlled by a finite number of movable points. The points control the deformation by Bernstein polynomials. In contrast to our approach, the control points have to be arranged on a regular grid. Furthermore, their influence is less immediate so that the result of the deformation is harder to estimate. Global mathematical mappings like e.g. those used in [Buche, Camillerap, 1991] can only be used for small deformations or for deformations with a simple mathematical description.

In summary, the approach presented in this contribution has the following advantages:

- The control points can be chosen arbitrarily.
- The deformation is performed exactly at the control points.
- It is easy to control the global influence of local deformations.
- The methods are easily tailored to meet special requirements.

There are other classes of methods of scattered data interpolation not investigated here. One example are the FEM approaches based on triangulation of the given data points. FEM interpolation methods were not taken into consideration since they can be carried out well in $\mathbb{R}^2$ but become computationally expensive and hard to implement in higher dimensions, whereas the methods presented here seem easily extensible. The latter has still to be done, in particular in 3D space.

Each method of interpolation behaves like a deformable material with very own properties. These properties are more or less natural to the user and the given problem. The usefulness depends on the experience of the user who will typically be well acquainted with concrete physical materials, say like an elastic skin of rubber. If a method of interpolation behaves quite different the user may have troubles and may need some time to gain experience with the new material. Then, however, this non-conventional method might be even better suited for solving the given problem of deformation than any real material may be. Nevertheless, a task of further work is to design and implement methods of deformation derived from physical laws.

References

[1] P. Alfeld. Scattered data interpolation in three or more variables. In T. Lyche and L.L. Schumaker, editors, *Mathematical Methods in CAGD*, pages 1–33. Academic Press, 1989.

[2] J.-D. Boissonat. Shape reconstruction from planar cross sections. *Computer Vision, Graphics, and Image Processing*, 44:1–19, 1988.

[3] P. Buche and J. Camillerapp. Serial cuttings matching: An application to muscle fiber characterization. In *Proceedings EuroGraphics '91*, pages 329–340, 1991.

[4] J. Duchon. Splines minimizing rotation invariant semi-norms in Sobolev spaces. In W. Schempp and K. Zeller, editors, *Constructive Theory of Functions of Several Variables, Lecture Notes in Math. Vol. 571*, pages 85–100. Springer Verlag, 1977.

[5] M. Eck. Interpolationsmethoden zur Rekonstruktion von 3D-Oberflächen aus ebenen Schnittfolgen. *CAD und Computergraphik*, 13(5):109–120, February 1991.

[6] R. Farwig. Rate of convergence of Shepard's global interpolation formula. *Mathematics of Computation*, 46(174):577–590, 1986.

[7] R. Franke. Scattered data interpolation: Tests of some methods. *Mathematics of Computation*, 38(157):181–200, January 1982.

[8] R. Franke and G. Nielson. Smooth interpolation of large sets of scattered data. *Int. Journal for Numerical Methods in Engineering*, 15:1691–1704, 1980.

[9] W.J. Gordon and J.A. Wixom. Shepard's method of "metric interpolation" to bivariate and multivariate interpolation. *Mathematics of Computation*, 32(141):253–264, 1978.

[10] B. Guenther. A system for simulating human facial expression. In N. Magnenat-Thalmann and D. Thalmann, editors, *State-of-the-art in Computer Animation*, pages 191–202. Springer Verlag, 1989.

[11] R.L. Hardy. Multiquadric equations of topography and other irregular surfaces. *Journal of Geophysical Research*, 76(8):1905–1915, 1971.

[12] P. Lancaster and K. Salkauskas. Surfaces generated by moving least squares methods. *Mathematics of Computation*, 37(155):141–158, 1981.

[13] T.W. Sederberg and S.R. Parry. Free-form deformation of solid geometric models. *Computer Graphics*, 20(4):151–160, 1986.

[14] D. Shepard. A two-dimensional interpolation function for irregularly spaced data. In *Proc. 23 Nat. Conf. ACM*, pages 517–524, 1968.

[15] G. Wolberg and T.E. Boult. Separable image warping with spatial lookup tables. *Computer Graphics*, 23(3):369–378, 1989.